Limnol. Oceanogr., 51(4), 2006, 1716–1728

Photo-oxidation of dissolved organic matter in river water and its effect on trace element speciation

Alan M. Shiller
Department of Marine Science, University of Southern Mississippi, Stennis Space Center, Mississippi 39529

Shuiwang Duan[1]
Department of Earth and Environmental Sciences, Tulane University, New Orleans, Louisiana 70118

Peter van Erp
Department of Marine Science, University of Southern Mississippi, Stennis Space Center, Mississippi 39529

Thomas S. Bianchi[2]
Department of Earth and Environmental Sciences, Tulane University, New Orleans, Louisiana 70118

Abstract

To investigate the effect of photodegradation of fluvial dissolved organic matter (DOM) on dissolved trace element distributions, we performed a 3-week incubation of water from the lower Pearl River (Mississippi). The experiment was performed in natural light (with dark controls) and examined both the changes in DOM and changes in physical–chemical speciation of a suite of trace metals. During the incubation, dissolved organic carbon (DOC) decreased in the light by about 20%, whereas ultraviolet light absorbance decreased by nearly 40%; dark controls showed no significant change in DOC. For the trace elements, a variety of behaviors were observed. Some elements (alkali and alkaline earth metals, Mo, Mn, Cd, and Zn) showed no change in concentration or speciation. A number of elements, however, did show significant changes in the light. For example, there was a significant, continuous decrease in dissolved (<0.02-μm) Fe in the light samples during the experiment. This and other speciation results indicate that organically complexed Fe was released during photo-oxidation of the low-molecular-weight DOM; this was followed by subsequent precipitation of the released Fe as additional colloidal FeOOH. Other elements (Ce, Cu, Cr, Pb, V, and U) also showed decreases in the dissolved (<0.02-μm) fraction with time. Some of these elements, as well as Co and Ni, also showed decreases in their retention by an anion exchange column, likewise implying a decrease in their organically complexed forms.

Photodegradation of dissolved organic matter (DOM) has been shown to be a significant or even dominant mechanism of oxidation of this material in sunlit waters (e.g., DeHaan 1993; Molot and Dillon 1997; Kohler et al. 2002) with concomitant contributions to increases in dissolved inorganic carbon (DIC) (e.g., Miller and Zepp 1995; Kohler et al. 2002) and nutrients (e.g., Bushaw et al. 1996; Tarr et al. 2001) as well as production of smaller, labile, biologically available organic compounds (e.g., Kieber et al. 1990; Wetzel et al. 1995). Photochemistry has also been shown to be an important aspect of the cycling of certain trace elements, particularly iron (e.g., Miles and Brezonik 1981; Voelker et al. 1997; Emmenegger et al. 2001). One interesting contrast in the studies of photochemical effects on DOM versus Fe is the difference in timescales generally considered. For DOM, the timescale for photodegradation in natural sunlight appears to be days to weeks in river waters (e.g., Kohler et al. 2002) and even longer in ocean surface waters (e.g., Moran and Zepp 1997). However, for Fe, photochemical effects can be apparent in diel redox cycling of Fe(II) (e.g., Collienne 1983; Emmenegger et al. 2001). Nonetheless, given that complexation by dissolved organic carbon (DOC) is an important factor in the mobilization of certain trace elements as well as in the redox cycling of Fe (Theis and Singer 1974; Voelker and Sulzberger 1996; Voelker et al. 1997), it is reasonable to suspect that long-term (i.e., days to weeks) photodegradation of DOC will lead to changes in metal complexation and hence dissolved-particulate partitioning with time. Stated another way, one might hypothesize that, for metals in rivers, the main effect of light on the short term is to effect changes in metal oxidation state, whereas on the long term the main effect of light is to alter metal complexing organic matter. Indeed, if the photoreactive components of DOM are important in fluvial metal complexation, then DOM photodegradation could

[1] Present address: Department of Marine Science, Texas A&M University at Galveston, Galveston, Texas 77551.

[2] Present address: Department of Oceanography, Texas A&M University, College Station, Texas 77843-3146.

Acknowledgments

We thank Lyndsie Gross for help in the field and the lab, Bryan Grace for assistance with HPLC analyses of amino acids, and Steve Lohrenz for lending his incubators. The manuscript was improved by comments from two anonymous reviewers. Support was provided by the National Science Foundation (EAR-0001286 and EAR-0001049).

lead to fundamental differences in metal speciation, transport, and bioavailability between low-order streams with fresh allochthonous carbon inputs and floodplain rivers dominated by photorefractory organic carbon.

An examination of previous work suggests uncertainty regarding the effect of photodegradation on the ability of organic matter to complex metal ions. Barbeau et al. (2003) showed that photolysis of Fe(III)-siderophore complexes in seawater can lead to the formation of lower affinity Fe-complexing ligands or result in no change in binding strength, depending on the particular Fe-binding moiety. In natural seawater samples, Powell and Wilson-Finelli (2003) found that, although exposure to sunlight resulted in a decrease in the amount of strong Fe-binding ligands, there was no change in ligand binding strength. Both the Barbeau et al. (2003) and Powell and Wilson-Finelli (2003) experiments were conducted short term (<1 d) in natural sunlight. These experiments indicate that there can be rapid photochemical degradation of certain strong Fe chelators. However, given that conditional stability constants for Fe–organic complexes in seawater are significantly greater than Fe–humic conditional stability constants in river water (e.g., compare the reviews of Gaillardet et al. 2003 with Bruland and Lohan 2003), these short-term seawater experiments say little about longer-term effects of light on the general metal complexation capacity of fluvial DOM. (This contrast in stability constants should hold true even when accounting for differences in side reaction coefficients between seawater and freshwater.)

Xie et al. (2004) examined the photodegradation of DOM from rivers of differing pH and DOC concentrations using 46-h incubations in high intensity (11× sunlight) light. They observed that the absolute concentration of carboxyl groups did not change substantially during irradiation experiments even while the DOC concentration significantly decreased. Xie et al. (2004) did not examine changes in metal–organic complexation. However, because carboxyl groups appear to play an important role in metal–organic complexation in natural waters (e.g., Reuter and Perdue 1977), their results suggest that loss of complexing capacity during DOM photodegradation might not be as great as loss of DOM.

Patel-Sorrentino et al. (2004) determined the Cu-complexing ability of Amazon River DOM before and after a photo-incubation. They found an increase in Cu-complexing ability following 20-min exposure to high-intensity (30× sunlight) light and suggested that this could result from a conformational change that exposed previously inactive complexing sites. In contrast, Lindim et al. (2000) examined Pb speciation in an irradiation experiment utilizing filtered salt marsh water from the highly contaminated Tagus River estuary (28 nmol L^{-1} Pb). During a 10-d exposure to ultraviolet B (UV-B) light with an intensity and day/night period similar to natural sunlight, they observed substantial decreases in Pb ligand concentrations, although most Pb was still complexed by organic matter by the end of the experiment. In addition, Sander et al. (2005) exposed alpine lake water to high-intensity UV-B radiation for a week. Although they observed a significant decrease in the concentration of Cu-complexing ligand during the incubation, their estimate of the rate of ligand destruction under natural conditions suggested that photodegradation of the Cu ligand was not a significant factor in the lake environment.

Because of their short durations, use of high-intensity light, or reliance on samples from contaminated environments, none of the experiments described above can be directly applied to predicting what happens to natural metal speciation during DOM exposure to sunlight over the course of the many days or weeks that it can take for low-order stream waters to reach the flood plain. Nonetheless, these previous results indicate that further examination of the relationship between DOM photodegradation and metal speciation is warranted.

Here, we present the results of a combined carbon–metal photo-incubation study using water from a river with inputs of carbon from soils, wetlands, and agricultural activity. The basic goal of the study was to examine whether changes in metal speciation are observed over timescales of days to weeks and to see the extent to which those changes are correlated with changes in DOM and its properties (e.g., DOC, dissolved organic nitrogen [DON], and UV absorbance).

Methods

The incubation experiment took place over a 3-week period from 19 February to 11 March 2004. Water for the experiment was collected from the Pearl River along the Mississippi–Louisiana border near the Stennis Space Center, Mississippi (30°21.57′N, 89°39.49′W). The Pearl is a small, circum-neutral, blackwater river with low suspended load. At the time of sampling (18 February 2004), there was substantial overbank flooding of the surrounding wetlands due to heavy recent rains.

In designing a 3-week-long photo-incubation experiment, we desired to eliminate or at least minimize biological effects. However, this is problematic. Addition of poisons, as well as heat and ultrasonic sterilization, can affect abiotic as well as biological processes (e.g., Shiller and Stephens 2005). Organic poisons also complicate the determination of DOC. Use of a high-intensity light source can obviate the need for a biological poison by greatly increasing the rate of photochemical processes relative to biological processes. However, such an approach may provide unrealistic results if important secondary inorganic reactions become slow relative to primary photochemical processes or if rates are affected by sample heating by the high-intensity light source.

Another approach is to use sterile filtration. The potential problem with sterile filtration is that it eliminates suspended particles, which can be an important reservoir of desorbable and dissolvable trace elements, and also it may not entirely eliminate small bacteria. Nonetheless, sterile filtration through 0.22-μm cartridge filters was the approach chosen for this experiment, because preliminary observations of a low suspended load and a large amount of colloidal Fe in Pearl River water suggested that filtered water could still provide a reasonable approximation of Pearl River water chemistry. Although neither bacterial

production nor biomass was determined during the incubation experiment, we recognize that there was undoubtedly some level of microbial activity in our experimental aliquots. Nonetheless, evidence from other analyses indicates that the effect of residual bacterial activity was minor. This evidence is presented below in our discussion but can be summarized as follows: (1) no dark DOC removal over 3 weeks, (2) no production of nonprotein amino acids (NPAAs), and (3) no oxidative removal of Mn.

During the initial sample collection, river water was pumped through acid-washed Teflon tubing using an acid-rinsed Teflon diaphragm pump. The water was filtered in-line through a 5-μm cartridge filter (Pall-Gelman Groundwater Sampling Capsule; Versapor/polypropylene) followed by a 0.22-μm cartridge filter (Whatman Polycap 150 TC; polyethersulfone/polypropylene) and then held in a 50-liter polyethylene carboy. The cartridge filters and carboy were acid washed and then rinsed first with ultrapure water and then filtered river water. Cartridge filters were changed after filtering 10–15 liters of river water. Because of filter clogging during the filtration process, it is probable that the effective pore size for filtration was somewhat smaller than 0.22 μm.

After returning to the laboratory, approximately 2-liter aliquots were placed into 20, 5-liter acid-washed 127-μm thickness Teflon FEP bags (Berghoff). Each bag was rinsed with some of the filtered river water. The FEP bags were chosen for their cleanness both for trace elements and DOC as well as for their relative UV/visible transparency. For instance, at 254 nm, the bags transmitted >80% of the incident light. The openings of the bags were folded over several times and taped shut. One-half of the bags were placed in a dark laboratory incubator held at 20°C. The other half of the bags were suspended in two water-filled Plexiglas incubators kept outdoors in ambient sunlight. The outdoor incubators were also temperature controlled at 20°C. At one point during the incubation, temperature control of the outdoor incubators was lost, and the water temperature rose several degrees for about half a day.

The daily length of visible light varied from 12.0 to 12.7 h during the experiment. The sky was generally clear the first 4 d of the experiment, followed by 13 d of mainly overcast skies with periods of cloudiness and clearing, and then the final 6 d were clear. Solar irradiance was not measured during the experiment; calculations indicate that daily solar insolation would have been ~30 MJ m^{-2} during the experiment (Kirk 1994).

Approximately every 5 d during the incubation, two "dark" bags and two "light" bags were taken for sample processing. The bags were chosen randomly to ameliorate possible bias due to position placement in the incubators. An initial sample was also collected. From each sample, between 100 and 350 mL were used for immediate trace element filtration and chemical fractionation. Also, a 25-mL aliquot was placed in an acid cleaned and precombusted (450°C) amber 40-mL glass vial and acidified with addition of 100 μL of ultrapure 2 mol L^{-1} HCl to remove inorganic carbon. The rest of the water was then placed in acid-cleaned polyethylene bottles and frozen prior to DOC analysis and characterization.

The taking of samples for processing was done midday to avoid possible bias due to diel effects on the cycling of Fe or other metals. Although Fe(II) was not determined in this experiment, other observations indicate that Fe(II) is a small percentage of total Fe in the Pearl River (20–80 nmol L^{-1} in <0.02-μm samples and 50–140 nmol L^{-1} in <0.45-μm samples; van Erp and Shiller unpubl. data). This low percentage of Fe(II) is consistent with other work in circum-neutral freshwaters (e.g., Emmenegger et al. 2001) and suggests that sample collection could have been performed at any time without significant bias for our experimental purposes.

For trace element analysis, three types of samples were saved. First, from each incubation bag, a 15-mL unfiltered sample was placed in a small acid-cleaned polyethylene bottle and acidified to pH < 2 with 70 μL of ultrapure 6 mol L^{-1} HCl (Seastar). This sample served as a check on loss of metal due to adsorption onto the walls of the incubation bags. Total concentrations of all trace elements in both the light and dark bags did not vary significantly during the course of the experiment, and thus we conclude that there was no loss of total metal concentrations to the walls of the incubation bags.

Second, from each incubation bag, a 15-mL sample of water filtered through a 0.02-μm syringe filter (Whatman Anotop; Shiller 2003) was also collected. This sample aliquot was similarly acidified and was saved for determination of dissolved (i.e., <0.02-μm) trace element concentrations.

Finally, from half of the sample bags (i.e., one "light" bag and one "dark" bag every 5 d), we also processed ~240 mL of water using the trace element fractionation method of Jiann and Presley (2002). This speciation method uses columns of clean Chelex-100 and AGMP-1 to operationally separate trace elements into "labile" (i.e., Chelex-extracted) and "organic-bound" (i.e., AGMP-extracted) fractions, which are then eluted from the columns using small (~10 mL) quantities of ultrapure 2 mol L^{-1} HNO_3 (Seastar). Note that, for the initial sample, two aliquots were processed through the chemical fractionation columns. Also, unlike Jiann and Presley, we did not buffer our samples but ran them through the columns unadjusted. Because the water passes through the Chelex-100 column first and then the AGMP-1 column, the Chelex fraction contains metals found in weak (relative to Chelex-100) organic complexes. Chelex-100 has a size exclusion limit of ~3.5 kDa, which may result in some limitation on its extraction of metals from weak high-molecular-weight (HMW) complexes. The AGMP-1 resin has an exclusion limit somewhere above 100 kDa, indicating that the highest molecular weight fractions should pass through this column. As we discuss below, the AGMP-1 resin probably retained some colloidal components in addition to low- and high-molecular-weight organic complexes. Obviously, the Jiann and Presley method is operational in nature, but it has the advantage of being relatively simple to perform and able to provide speciation information for a wide sweep of elements.

These various subsamples were subsequently analyzed for a suite of trace elements by inductively coupled plasma–

mass spectrometry (ICP-MS) using a sector field instrument (Thermo Finnigan Element 2) with a low flow nebulizer (100 μL min^{-1}; Elemental Scientific). Samples were diluted (from 30% to 20-fold, depending on the element) with the addition of ultrapure dilute nitric acid (Seastar) with added internal standards (High Purity Standards). With this addition, samples are ~2 μg L^{-1} in Sc, In, and Th and 0.16 mol L^{-1} in HNO_3. Calibrations were performed using standards made in 0.16 mol L^{-1} nitric acid. Several samples were also calibrated by the method of additions. No significant difference was noted for the two calibration methods. Sample acidification and other preparations for analysis were carried out in a laminar flow clean bench. Detection limits were $\leq$1 pmol L^{-1} for Cs, Re, and Tl; $\leq$5 pmol L^{-1} for Cd, Ce, and U; $\leq$10 pmol L^{-1} for Pb; $\leq$0.1 nmol L^{-1} for Co, Cr, Cu, Mo, Ni, Rb, and V; $\leq$1 nmol L^{-1} for Ba, Li, Mn, Sr, and Zn; and $\leq$3 nmol L^{-1} for Al and Fe. Relative analytical precision for samples well above the detection limit was typically $\pm$5% (1σ).

Hydrogen peroxide concentrations were not measured in the incubation bags. Preliminary experiments indicated that the half-life of H_2O_2 in Pearl River water was less than half an hour and that organic matter severely interfered with the H_2O_2 determination, thus making the analysis of this photogenerated species problematic (Yuan 2000).

Samples for DOC and total dissolved nitrogen (TDN) were analyzed within a few days of collection. Both DOC and TDN measurements were performed on a Shimadzu TOC-VCSH/CSN analyzer using high-temperature catalytic oxidation (HTCO) and chemiluminescence, respectively. The precision for DOC ($\pm$4%) and TDN ($\pm$4%) analyses was estimated using a coefficient of variation (n = 3).

Half of the DOC samples (i.e., one light bag and one dark bag from each sampling date) were also processed by ultrafiltration. Specifically, low-molecular-weight (LMW) DOM was collected using an Amicon 8M Micro-Ultrafiltration System with 1-kDa regenerated cellulose membranes (Millipore) that had been cleaned by submerging the membranes in a 35 g L^{-1} NaCl solution that was changed daily for 1 week (Orem et al. 1986). Ultrafiltration was carried out by pressurizing the system with nitrogen (~400 kPa), which allowed water containing the LMW DOM (<1 kDa) material to pass through the membrane, producing a final volume of ca. 4 mL. The samples were diluted to 10 mL using ultrapure water and acidified prior to DOC analysis. Processing of blanks indicated that carbon contamination to the system was typically less than 7% between the retentate and the filtrate.

Ultraviolet/visible (UV/VIS) spectra of filtered samples were measured using a 1601 UV/VIS spectrophotometer (Shimadzu); dissolved Fe was low enough in our samples to be only a minor interferent in the light absorbance measurements (e.g., Weishaar et al. 2003).

Amino acids were analyzed using high-performance liquid chromatography (HPLC) after pre-column *O*-phthaldialdehyde (OPA; Sigma) derivatization, according to the method of Lee and Jørgensen (1995). The analysis of total dissolved amino acids (TDAA) was performed after hydrolysis with 6 mol L^{-1} HCl (containing 0.5% phenol) in nitrogen atmosphere at 110°C $\pm$ 2°C for 24 h (Cowie et al. 1992); dissolved combined amino acid (DCAA) concentration was obtained by difference between dissolved free amino acid (DFAA) and TDAA concentrations. An Alltech Alltima C_{18} (5 μm; 250 $\times$ 4.6 mm) column was used with a flow rate of 0.95 mL min^{-1}. All HPLC analyses were performed on a Dionex GP-50, coupled with an ASI-100 refrigerated autosampler (Dionex), using a binary gradient. Mobile phase A consisted of a sodium acetate buffer (0.05 mol L^{-1} sodium acetate with 5% tetrahydrofuran, pH 5.4–5.7, adjusted with acetic acid), while mobile phase B was 100% HPLC-grade methanol. The HPLC gradient at time zero began with 22% of B, then ramped to 60% B in 40 min, and finally 100% B in 50 min, where it remained isocratic for an additional 10 min. Fluorescence emission and excitation wavelengths were set at 330 and 418 nm, respectively, on a Dionex RF 2000 fluorescence detector. A Pierce Chemical protein amino acid mixture was used as a standard for most of the amino acids, excluding the nonprotein forms. Known amounts of the nonprotein amino acids β-alanine, γ-aminobutyric acid (Sigma Chemical), and 5-aminovaleric acid (Aldrich Chemical) were added to the Pierce standard during preparation of standard solutions. Amino acids were identified based on retention times of authentic standards. Norvaline (Aldrich Chemical) was used as a recovery standard during the hydrolysis procedure.

In the discussion following, we refer to the <1-kDa DOM and <0.02-μm trace element samples as "low-molecular-weight" (LMW) or "dissolved" fractions, with the realization that there is a difference between our DOM and trace element size cutoffs. This difference was necessitated by the differing equipment cleanup requirements for organic carbon and trace element samples.

In evaluating the incubation data, a *t*-test was applied to concentration versus time relationships. Concentration changes are labeled as significant (*see Table 1*) for $p <$ 0.05 as long as the relative change in concentration during the incubation was >5%.

Results and discussion

Dissolved organic carbon—For DOC, the dark-bag concentrations did not change significantly during the incubation, either in total concentration or in the low-molecular-weight fraction (Fig. 1). Also, in the dark bags, light absorbance at 365 and 438 nm did not vary; and at 254 nm, light absorbance decreased by <4% (Fig. 2).

In contrast, in the light bags, DOC decreased linearly by about 20% (Fig. 1) and light absorbance decreased by 37, 39, and 24% at 254, 365, and 438 nm, respectively (Fig. 2). Because absorbance at 254 nm decreased more rapidly than DOC concentration, this also means that specific UV absorbance (SUVA) decreased by 22% during the experiment. The decrease in SUVA in the light bags implies a decrease in the aromaticity of the DOC upon exposure to light (Chin et al. 1994; Weishaar et al. 2003). Because stability constants for metals with aromatic complexers tend to be higher than for similar aliphatic complexers (e.g., Martell and Smith 1995), the decrease in SUVA along with

Table 1. Summary of elemental speciation during incubation experiment. Elements are listed in the order discussed in the text.

	Initial elemental distributions					% change during incubation					
			% of total			Dissolved		Chelex		AGMP	
Element	Total (nmol L^{-1})	Dissolved (nmol L^{-1})	Diss.	AGMP	Chelex	Light	Dark	Light	Dark	Light	Dark
Fe	2,645	1,024	39	66	12	−45	n.s.	−66	−59	n.s.	ID−16
Pb	0.33	0.10	29	81	13	−44	n.s.	−71	−63	n.s.	ID−39
U	0.25	0.17	68	89	11	−15	17	Decr.?	ID?	−11	ID−11
Cu	21.6	18.3	85	86	11	−15	9	83	ID−22	−10	n.s.
Ce	12.8	7.7	60	92	4	−28	5	140	ID−32	−16	ID−13
Cr	3.4	2.4	72	93	3	−39	10	n.s.	n.s.	ID−13	ID−17
V	7.0	5.8	84	87	5	−15	n.s.	n.s.	n.s.	−15	−12
Co	2.2	1.9	87	36	51	n.s.	n.s.	46	n.s.	−83	n.s.
Ni	20.2	17.0	84	54	23	n.s.	n.s.	69	n.s.	−39	n.s.
Ba	142	126	89	0	102	n.s.	n.s.	n.s.	n.s.	n.s.	n.s.
Cs	0.023	0.019	83	3	82	n.s.	n.s.	n.s.	n.s.	n.s.	n.s.
Li	71	70	99	1	97	n.s.	n.s.	n.s.	n.s.	n.s.	n.s.
Rb	39	38	97	0	102	n.s.	n.s.	n.s.	n.s.	n.s.	n.s.
Sr	151	144	96	0	99	n.s.	n.s.	n.s.	n.s.	n.s.	n.s.
Cd	0.15	0.13	89	14	84	n.s.	n.s.	n.s.	n.s.	n.s.	n.s.
Mn	708	649	92	1	92	n.s.	n.s.	n.s.	n.s.	−27	n.s.
Tl	0.014	0.014	100	8	96	n.s.	n.s.	n.s.	n.s.	n.s.	n.s.
Zn	60	51	81	6	78	n.s.	n.s.	n.s.	n.s.	n.s.	n.s.
Mo	0.38	0.42	109	103	4	n.s.	n.s.	n.s.	n.s.	n.s.	n.s.
Re	0.002	0.002	100	80	2	n.s.	n.s.	n.s.	n.s.	n.s.	n.s.
As	4.3	3.6	83	68	0	n.s.	n.s.	n.s.	n.s.	n.s.	n.s.

* Decr., decrease; Diss., dissolved; ID, initial drop in concentration between experiment beginning and day 4 sample; n.s., no significant change.

the decrease in DOC may indicate a decrease both in the amount and strength of organic complexers.

The ultrafiltration data show that essentially all of the decrease in DOC in the light bags took place in the LMW-DOM fraction (Fig. 1). As will be discussed in the following, this is compatible with the physical–chemical speciation changes we observed in trace elements.

For the incubation experiment, the overall oxidation rate of organic matter in the light bags was 0.23 μmol C L^{-1} h^{-1}. Although the bacterial production rate was not determined in our initial unfiltered incubation sample, an in situ bacterial production rate in the Pearl River of 0.1 μmol C L^{-1} h^{-1} was observed in October 2001 (Duan, Shiller, and Bianchi unpubl. data). Thus, photochemical oxidation of DOM appears to occur at a rate similar to bacterial oxidation in this system. Also, this comparison of oxidation rates lends support to our argument that bacterial activity was a minor effect in our incubation experiment, because by removing bacterial biomass, the prefiltration of the incubation water would have resulted initially in an even greater contrast between photochemical and microbial carbon oxidation rates for our experimental aliquots.

The light absorbance data for the light bags indicates that the $a^{254} : a^{365}$ ratio did not change significantly, whereas the $a^{254} : a^{438}$ ratio decreased by 17% during the experiment. As summarized by Twardowski and Donaghay (2002), the usual expectation is that these ratios should decrease if the low-molecular-weight fraction is preferentially degraded; that is, the observed change in light absorbance ratios is in general accord with our ultrafiltration observations. Other workers have also used short-to-long wavelength absorbance ratios as a proxy for changes in molecular weight distribution of natural organic matter (e.g., DeHaan 1993; Osburn et al. 2001). However, in contrast to our results, many other experiments have found a greater proportionate photobleaching at longer wavelengths compared to shorter wavelengths (Twardowski and Donaghay 2002, and references therein). We do note that these previous experiments generally utilized either marine samples or humic-rich waters having DOC concentrations substantially greater than in the Pearl River. Interestingly, Gao and Zepp (1998), using Satilla River water, and Morris and Hargreaves (1997), using waters from several northeast Pennsylvania lakes, did find spectral slope decreases with increasing light exposure (i.e., results similar to ours). Clearly, these divergent results suggest that differences in DOC characteristics, experimental setup, or other factors such as Fe content (which can catalyze DOC photoreactions; e.g., Gao and Zepp 1998, and references therein) may result in somewhat different photoreactions.

For TDN and DCAA, the dark-bag concentrations did not change significantly (*t*-test, $p > 0.05$) during the incubation, but DFAA increased significantly (*t*-test, $p < 0.05$) by 20% (Fig. 3). The reason for the 20% increase in DFAA in the dark bags is not clear, and is the only exception we observed to the constancy of DOM parameters in the dark.

In contrast, in the light bags, both TDN and DCAA decreased significantly (*t*-test, $p < 0.05$) by 11% and 23%, respectively, whereas DFAA increased significantly (*t*-test, $p < 0.05$) by 38%, i.e., somewhat higher than the DFAA increase in the dark (Fig. 3). Most of these changes occurred during the first 12 d. The dominant DFAA found in the light treatment were glycine, serine, aspartic acid,

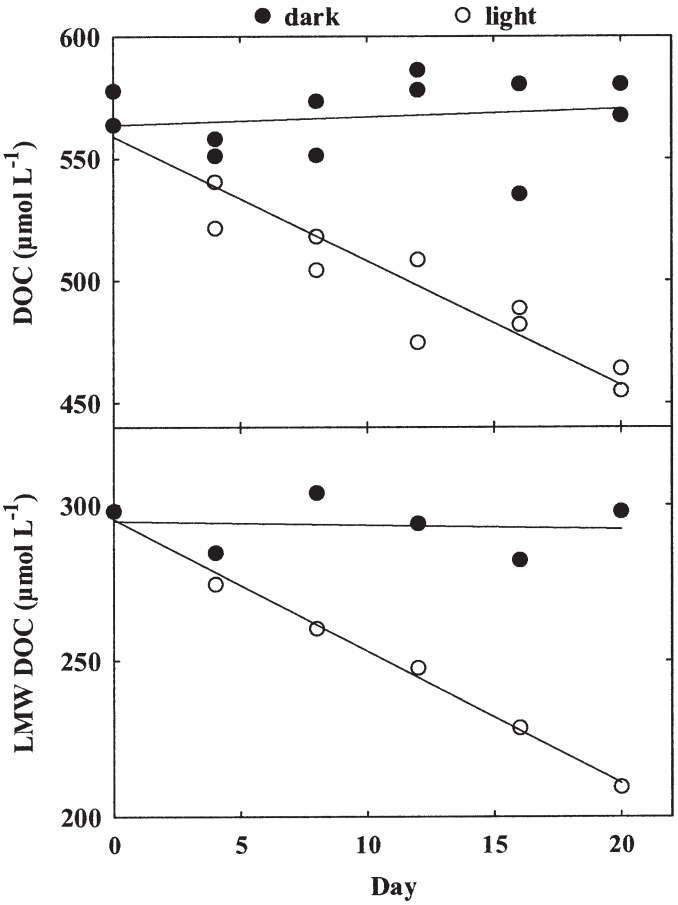

Fig. 1. Dissolved organic carbon (DOC) and low-molecular-weight (LMW) DOC (<1 kDa) in light and dark incubation bags.

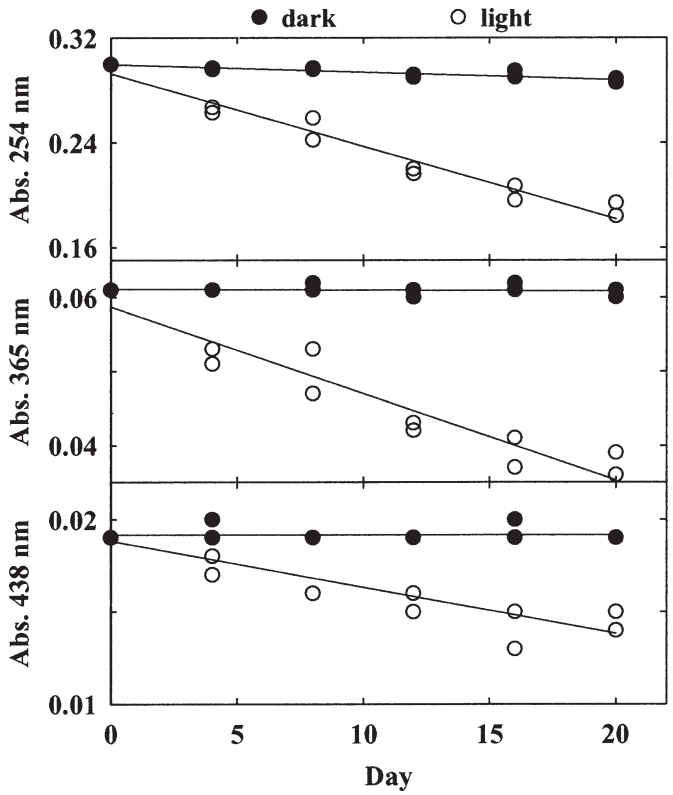

Fig. 2. Light absorbance (cm^{-1}) in light and dark incubation bags.

alanine, and valine. In the DCAA fraction of the light treatment, aspartic acid, glycine, and serine were the dominant amino acids. In the light treatment, a significant decrease in the abundance of the amino acids serine and glycine in the DCAA fraction was accompanied by an increase in these two amino acids in the DFAA fraction. In another study, serine was also observed to increase significantly with increasing photochemical breakdown of DOM (Tarr et al. 2001). Amino acid composition showed much less change in the dark bags except for a smaller increase in serine in DFAA. Because much of the DOM in the Pearl River is derived from soil humic substances, the release of amino acids as potential labile substrates is consistent with earlier studies. That prior work showed that photochemical transformation of humic-derived DOM rendered the material more biologically labile in contrast to the opposite effect on algal-derived DOM (Tranvik and Bertilsson 2001).

The 38% increase in DFAA, with decreasing DCAA, in the light bags suggests the release of free amino acids from DON when exposed to sunlight. The significant decrease in DCAA concentration in light bags in this study confirmed the breakdown of DON into DFAA or even perhaps dissolved inorganic nitrogen (DIN) (e.g., ammonium). Much of the photochemical breakdown of photochemical-labile DON occurred over the first 12 d. Because most of the decrease of DOC in light bags was attributed to oxidization of LMW DOM, the breakdown of small molecules of DON, such as DCAA, was likely responsible for the increase in DFAA. Although DIN was not measured in this study, photochemical release of ammonium from DOM has been shown in a number of studies (e.g., Bushaw et al. 1996; Tarr et al. 2001). If ammonium was the dominant form of photogenerated DIN, this might lead to loss of TDN by volatilization or adsorption onto the walls of the incubation bags. These changes in the abundance and/or composition of DOM during light exposure may also have affected the physical–chemical distribution of certain trace elements.

Another important observation in the amino acid data was that the NPAAs were not detectable above background noise. NPAAs such as β-alanine, α-aminobutyric acid, and ornithine are produced enzymatically during decay processes from precursors such as aspartic acid, glutamic acid, and arginine, respectively. Thus, elevated mole percentages of NPAA have been used as an index of organic matter degradation (Cowie and Hedges 1994; Keil et al. 1998). That we did not detect the NPAAs despite significant decreases in DOC and increases in DFAA lends confidence to our approach of using sterile filtration to minimize biological activity.

Iron—Fe is a key trace element due to its comparatively high concentration (>2.3 μmol L^{-1} total Fe in our experiments) and the fact that Fe oxyhydroxides can be

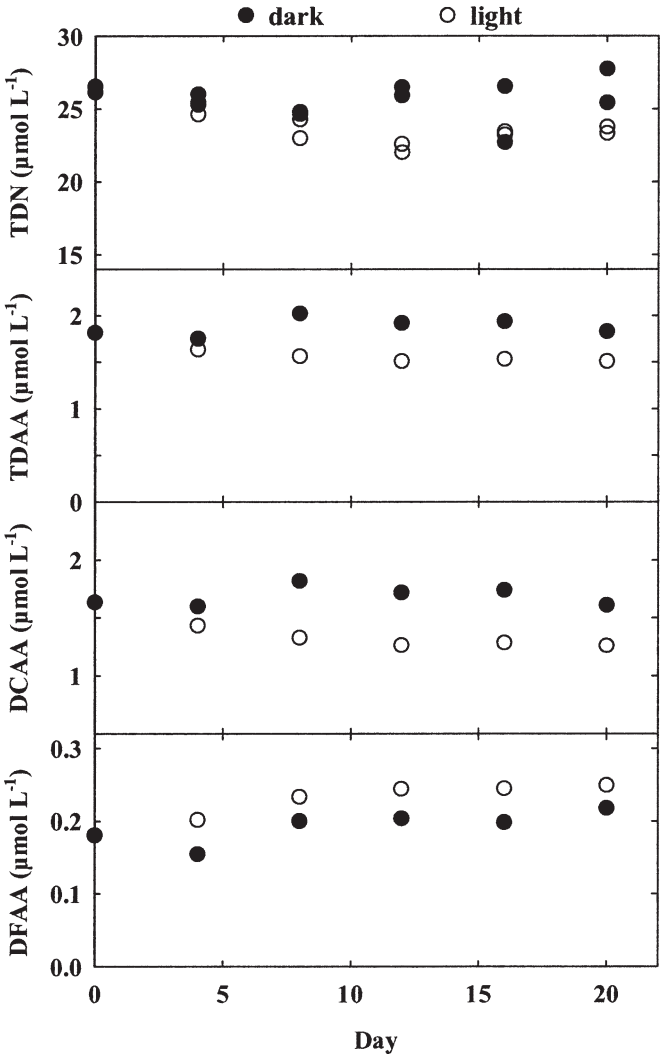

Fig. 3. Total dissolved nitrogen (TDN), total dissolved amino acids (TDAA), dissolved combined amino acids (DCAA), and dissolved free amino acids (DFAA) in light and dark incubation bags.

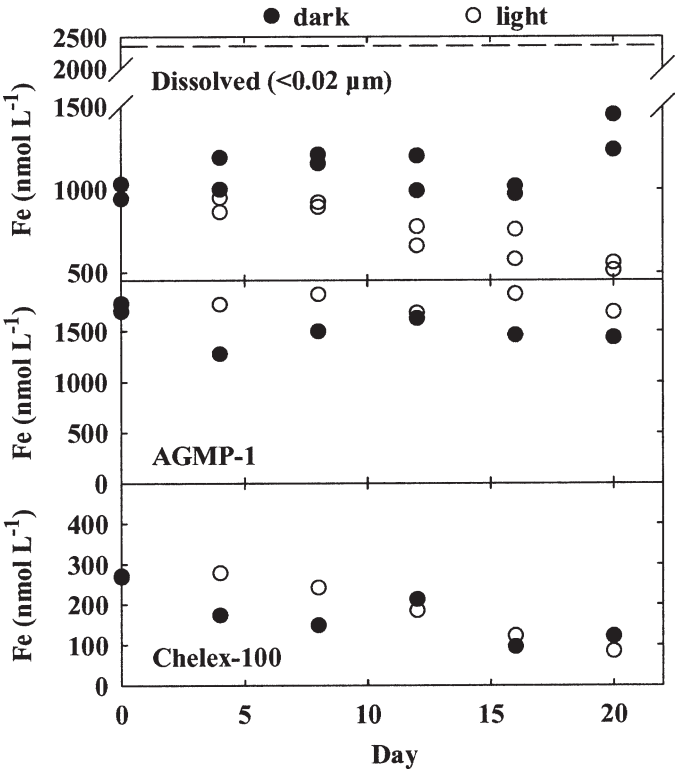

Fig. 4. Iron size and chemical speciation during incubation experiment. The dashed line in the top figure is total concentration (<0.22 μm).

important adsorbing surfaces in natural waters (e.g., Pokrovsky and Schott 2002). Additionally, as we have noted above, the diel photochemical cycling of this element has received much attention. Furthermore, the presence of Fe appears to catalyze the rate of photo-oxidation of DOC (e.g., Voelker and Sulzberger 1996; Gao and Zepp 1998).

At the pH of the Pearl River water in this experiment (6.4), inorganic Fe(III) solubility is <10 nmol L^{-1} (Liu and Millero 1999). Thus, Fe(III) in our incubation bags must either be complexed by organic matter or else in the form of colloidal FeOOH. As noted previously, other determinations of Fe(II) in the Pearl River indicate that most dissolved Fe in the river is oxidized Fe(III), not Fe(II). Oxidation of Fe(II) is probably very rapid in the Pearl River. A consideration of the rates of oxidation of Fe(II) by O_2, O_2^-, and H_2O_2 using rate constants from the literature (Rush and Bielski 1985; Millero and Sotolongo 1989; Millero et al. 1997) suggests that Fe(II) is predominantly oxidized by H_2O_2 in the Pearl River with a half-life of ~9 min. The oxidation rate estimates assume saturation with dissolved O_2 at 20°C, a steady-state O_2^- concentration of 0.8 pmol L^{-1} as estimated by the method of King et al. (1995), and 200 nmol L^{-1} H_2O_2 (Yuan 2000).

In the initial Pearl River water, Fe was found mainly (~61%) in the colloidal (0.02–0.2-μm) size range, although its dissolved (<0.02-μm) concentration was still significant (Fig. 4; Table 1). In the chemical fractionation, Fe was mainly extracted by AGMP-1 rather than Chelex-100 (Fig. 4). Because the AGMP-1 fraction for Fe was greater in concentration than the <0.02-μm fraction, this macroporous resin was extracting some amount of colloidal Fe (either HMW organic Fe or colloidal FeOOH).

In the dissolved (<0.02-μm) phase, there was a continuous ~450 nmol L^{-1} light-bag decrease in Fe during the incubation, whereas dark-bag Fe remained constant. (Despite the apparent increase in dark dissolved Fe at the end of the experiment, these dark-bag changes in Fe were not statistically significant.) These results are most simply explained by release of complexed Fe during photodegradation of the LMW organics followed either by precipitation of colloidal FeOOH or complexation by organic matter with a size greater than 0.02 μm.

In the AGMP-1 fraction, Fe remained constant in the light bags, whereas the dark bags showed a decrease of >200 nmol L^{-1} by day 4 and remained lower than in the light bags for the duration of the experiment. Because the AGMP-1 column appeared to retain both organic Fe as well as some colloidal Fe, the constancy of the AGMP-1

fraction in the light bags provides little information regarding the fate of the Fe released from oxidized LMW organics.

The initial decrease in AGMP-1-extractable Fe in the dark bags but not the light bags implies that a photochemical process producing a part of the AGMP-1-extractable Fe has been stopped in the dark bags. Because Fe in the <0.02-μm dark fraction did not show this same initial decrease, the AGMP-1 initial decrease must represent a dark loss of either colloidal FeOOH or HMW Fe complexes. Pb extracted by AGMP-1 showed a similar effect (Fig. 5). A study of trace element associations in a Swedish creek (Lyven et al. 2003) found Pb to be the one element most strongly associated with Fe rather than C colloids. Pokrovsky and Schott (2002) likewise found an association between Fe and Pb colloids in a number of small boreal rivers. Thus, the Pb result implies a dark loss of colloidal FeOOH. This is an unexpected result, because it is well established that light can photoreduce colloidal FeOOH (e.g., Waite and Morel 1984). We offer the hypothesis that photoredox cycling of Fe results in small-sized colloidal FeOOH, which can be retained by the macroporous AGMP-1. When this photoredox cycle is stopped, ageing/coagulation of small FeOOH colloids results in the formation of larger FeOOH particles that are no longer retained by AGMP-1.

In both the light and dark bags, the Chelex-100-extractable Fe showed a significant and steady decrease of $\sim$200 nmol L^{-1}. Because the <0.02-μm dark fraction did not decrease, the change in Chelex-extractable Fe most likely occurred in weak HMW complexes. Pb, which unlike Fe is not prone to oxidation, showed a similar decrease in light- and dark-bag Chelex-100 extraction (Fig. 5). This suggests that we are not simply observing a slow oxidation of complexed Fe(II). Note that, if Fe was slowly lost from HMW complexes, the associated increase in LMW Fe would probably not be evident in the scatter of our dark dissolved (<0.02-μm) results and would offset part of the light-bag dissolved Fe loss.

With the Chelex results indicating a loss of Fe from weak HMW complexes, there is also an implication for the loss of Fe from the dissolved fraction in the light bags. If the Fe lost from the light-bag dissolved fraction were transferred to HMW organic complexes, then we might expect Chelex-extractable Fe to change differently in the light and dark bags. (If HMW-Fe complexes are formed when Fe is released from LMW complexes, these new HMW complexes would necessarily have to be weaker than the original LMW complexes; otherwise, the Fe would have originally been in the HMW complexes.) Thus, the similar change in both light- and dark-bag Chelex-extractable Fe indicates that, when Fe was released by the photodegradation of the LMW organic matter, the Fe was transferred to colloidal FeOOH (rather than HMW organic complexes).

An obvious question is whether a change in colloidal FeOOH would be large enough to affect the distributions of other particle-reactive trace elements in Pearl River water. Dzombak and Morel (1990) argue that the adsorption properties of hydrous ferric oxide can be modeled by two adsorption sites, a strong affinity site that has a density of 0.005 mol site:mol Fe and a weak affinity site that has a density of 0.2 mol site:mol Fe. Thus, for only a 100 nmol L^{-1} change in colloidal Fe, one would expect a change of 0.5 nmol L^{-1} strong affinity sites and 20 nmol L^{-1} weak affinity sites. From the changes in the Fe distribution shown in Fig. 4 and the concentrations of other trace elements shown in Table 1, some effect on other trace elements is therefore a reasonable expectation. We address this further in the sections following.

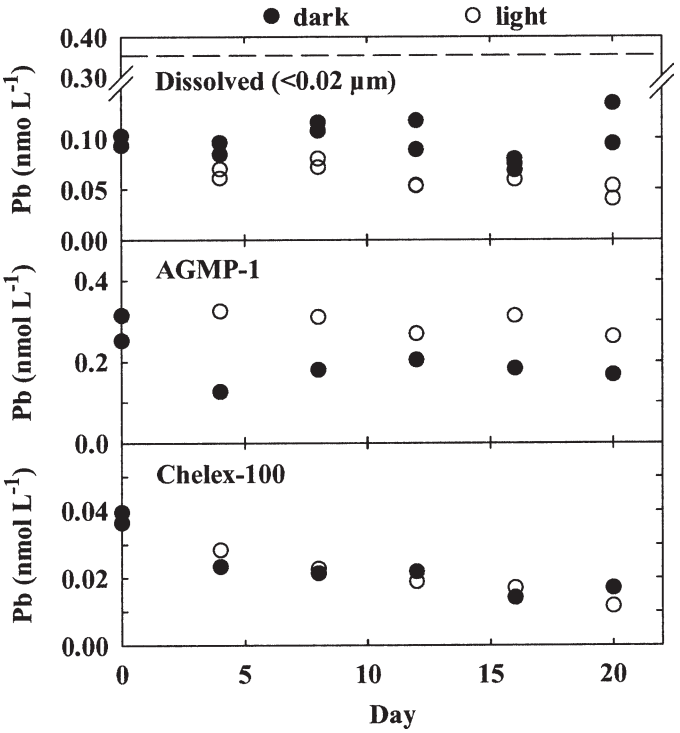

Fig. 5. Lead speciation during incubation experiment. The dashed line in the top figure is total concentration (<0.22 μm).

Our experimental results also suggest an interesting contrast between the diel and days-to-weeks timescales for Fe cycling in the Pearl River. The Fe(II) oxidation rate estimated above is roughly 100 times faster than the rate of removal of dissolved Fe we observed during the incubation. Thus, there was far more cycling of Fe between oxidation states in the light bags than there was transfer of Fe from the dissolved to the colloidal phase due to DOM photodegradation. Indeed, during the course of our 3-week incubation, each Fe atom in the system could have cycled between Fe(II) and Fe(III) over 10 times. Nonetheless, because Fe(II) is such a small percentage of total Fe in the system (dissolved or colloidal), the diel redox cycling of Fe probably alters the Fe speciation by no more than 5%. We offer the hypothesis that, from a trace element perspective, a major effect of diel photoredox cycling of Fe may be to maintain FeOOH surfaces as a freshly precipitated, high specific surface area hydrous ferric oxide rather than an aged, lower specific surface area goethite. In contrast to this, the long-term DOM degradation in our experiment decreased dissolved Fe by 45%. This far greater effect on speciation (despite a lower molar rate than ferrous

oxidation) results from organic ligand availability being the major control on dissolved Fe solubility.

Other elements showing a change in speciation—A number of other elements (Ce, Cu, Cr, Pb, V, and U) showed significant decreases in their dissolved (<0.02-μm) fractions during the incubation experiment. Additionally, Co and Ni showed changes in their chemical partitioning during the experiment. The behavior of these elements is summarized in Table 1; only graphs of selected example behaviors are shown. Interestingly, many of these elements were previously found to be associated with colloidal Fe in a study of small boreal rivers in Russia (Pokrovsky and Schott 2002), although some also showed a substantial association with organic colloids in a Swedish creek (Lyven et al. 2003). These elements can be further subdivided based on the behavior of their chemical fractionation during the experiment.

Lead and uranium—For Pb, there is substantial correspondence to Fe in initial size and chemical distributions (Table 1). This is not surprising given that a study of colloidal elemental associations in a Swedish creek (Lyven et al. 2003) found Pb to be the one element most strongly associated with Fe rather than C colloids. Pb was initially 70% in the colloidal size range, and in the chemical extraction ~80% was retained by AGMP-1 (Table 1), again implying retention of some fraction of colloidal FeOOH with associated Pb by the AGMP-1.

As was mentioned in the Fe section, changes in the Pb size and chemical fractions also paralleled the changes in Fe (Fig. 5). Thus, we conclude that photodegradation of organic matter resulted in transfer of Pb from the dissolved phase to colloidal FeOOH. One interesting additional insight from the Pb results comes from the drop in dark-bag AGMP-1-extractable Pb between the initial sample and day 4. This drop (~0.1 nmol L^{-1}) is larger than the entire amount of dissolved (<0.02-μm) Pb (which did not significantly change in the dark). Thus, this change in the dark AGMP-1 fraction must have resulted from changes entirely in the colloidal/HMW Pb fraction.

For U, this element in the initial sample was largely (68%) in the dissolved phase and most of it was extracted by the AGMP-1 column. Unfortunately, the first day's Chelex-100 extractions appear to have been contaminated for U.

In the light bags, there was a ~15% (~0.025 nmol L^{-1}) steady decrease in dissolved U during the incubation. The light-bag AGMP-1 fraction appears to have decreased by a similar amount. The light-bag Chelex-100-extractable U showed a ~0.015 nmol L^{-1} decrease (after day 4).

In the dark bags, dissolved U showed a scattered ~0.02 nmol L^{-1} increase. The dark-bag AGMP-1 fraction showed an initial drop followed by a more steady trend towards the light-bag values. Likewise, the Chelex-100-extractable U shows a slight (~0.01 nmol L^{-1}) decrease from days 4 to 20, but was always >0.02 nmol L^{-1} lower than the light-bag Chelex-100 U, again implying an initial drop in the dark bags.

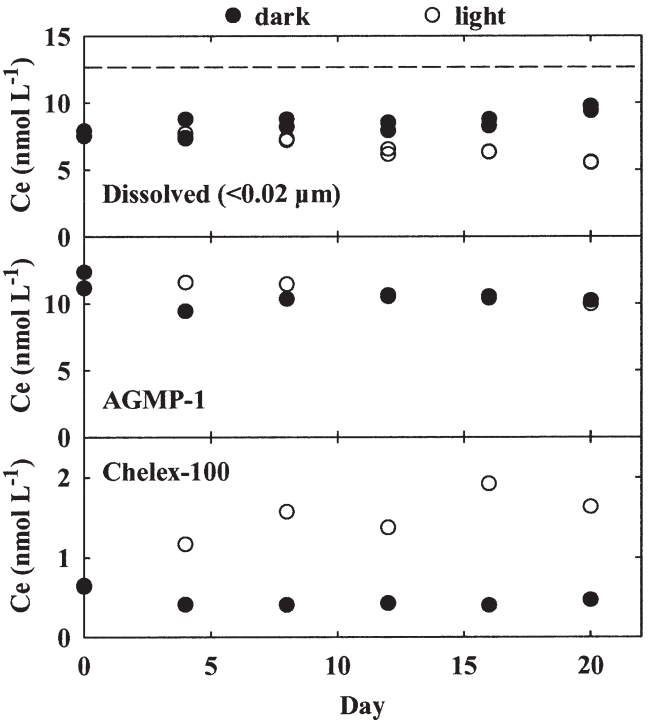

Fig. 6. Cerium speciation during incubation experiment. The dashed line in the top figure is total concentration (<0.22 μm).

Overall, the changes in U were small but are compatible with a slight transfer from dissolved to colloidal phase during the photodegradation of LMW organic matter.

Cerium and copper—Like iron, Cu and Ce showed measurable decreases in their light-bag dissolved concentrations during the experiment, although their dark-bag dissolved concentrations slightly increased with time (Figs. 6, 7). Both elements also were dominantly extracted by the AGMP-1 resin, again like Fe. However, in the Chelex-100 extraction, these two elements showed increases in their light-bag concentrations with time, whereas their dark-bag chemical distributions showed proportionately smaller initial decreases.

In the light bags, dissolved Ce decreased by ~4 nmol L^{-1} during the experiment, AGMP-1-extractable Ce decreased by ~2 nmol L^{-1}, and Chelex-100-extractable Ce increased by 1.5 nmol L^{-1} (Fig. 6). For Cu, the light-bag behavior during the experiment was similar to that observed for Ce, with a 2.8 nmol L^{-1} decrease in the dissolved fraction, a 1.6 nmol L^{-1} decrease in the AGMP-1 fraction, and a 1.1 nmol L^{-1} increase in the Chelex-100-extractable fraction (Fig. 7). The implication, then, is that photochemical oxidation of LMW DOC causes a release of these two elements mainly from strong complexes with a transfer to weakly bound (i.e., Chelex-100-extractable) and colloidal forms.

For Cu, the minimal changes in the dark bags is interesting given that there is evidence of photochemical involvement in the cycling of Cu between the dominant Cu(II) and reduced Cu(I) oxidation states (e.g., Moffett and Zika 1988). The implication of our dark-bag result is

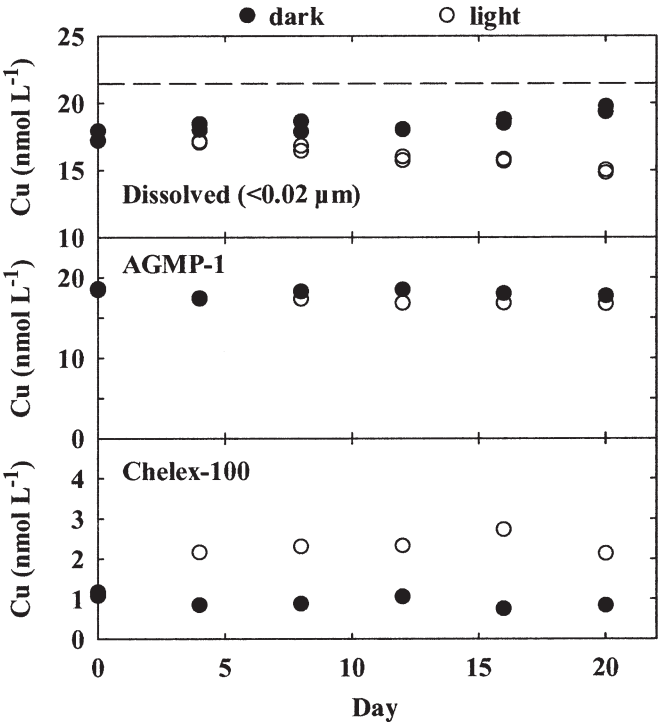

Fig. 7. Copper speciation during incubation experiment. The dashed line in the top figure is total concentration (<0.22 μm).

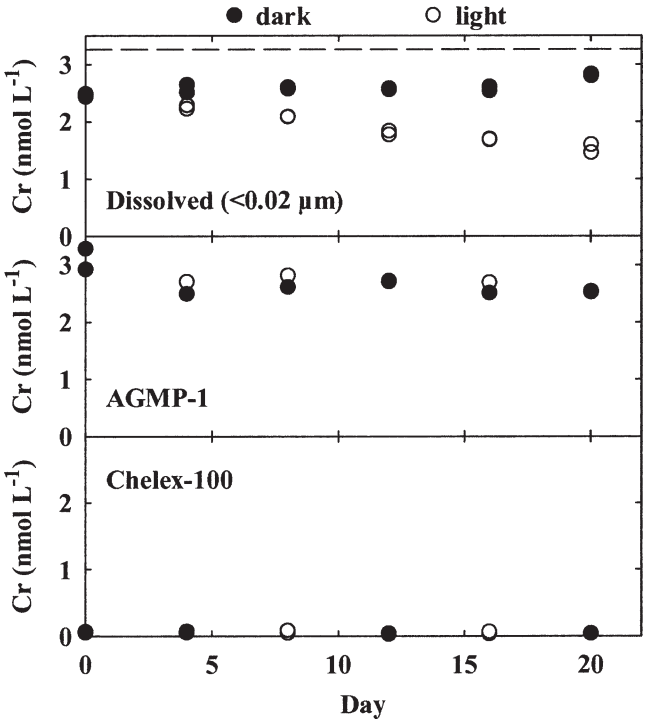

Fig. 8. Chromium speciation during incubation experiment. The dashed line in the top figure is total concentration (<0.22 μm). (Note that dark- and light-bag Cr concentrations values for Chelex-100 extraction were nearly identical on all days.)

that any diel photochemical cycling of Cu between these oxidation states did not substantially affect the steady-state size or chemical fractionation of this element in our experiment.

Chromium and vanadium—Cr also showed significant removal from the dissolved phase in the light bags, whereas the dark-bag size fractionation appeared to increase slightly (Fig. 8). For V, the size fractionation results were scattered in both the light and dark bags, but by the end of the experiment the light-bag dissolved V had decreased ~1.5 nmol L^{-1} (>20%), whereas the dark bags had not changed significantly. These two elements were almost entirely extracted by AGMP-1, which may simply be a reflection of a dominance of anionic speciation as chromate and vanadate. (Because Cr and V were so low in the Chelex-100 fraction [~0.05 and 0.4 nmol L^{-1}, respectively], no trends were evident in that fraction.) The AGMP-1 did initially extract ~0.7 nmol L^{-1} more Cr than there was in the dissolved phase (2.4 nmol L^{-1}), again implying some colloid extraction by this column. Indeed, about 30% of the total Cr was in the colloidal phase. The transfer of dissolved Cr and V to the colloidal phase in the light bags suggests two possible photochemical processes. That is, complexed Cr and V could be released from photo-oxidized organics and adsorbed onto colloidal Fe oxyhydroxides, or alternatively adsorption of dissolved Cr and V could occur on fresh colloidal Fe created by the release of complexed Fe during photo-oxidation of DOC.

For both Cr and V, the AGMP-1-extractable fraction decreased ~15% during the experiment in both the light and dark bags, implying a non-photochemical process. For Cr, the decrease came entirely between the first two samples; for V, about half of the decrease occurred initially, followed by a slower steady decrease during the rest of the experiment. Such a decrease could result from reduction of the anionic forms (by organic matter?) to Cr(III) and V(IV). However, this explanation is not especially appealing given that Cr(III) and V(IV) (as the VO^{2+} ion) would likely be either adsorbed by colloidal Fe oxyhydroxides (and hence appear as a decrease in the dissolved phase in both light and dark bags) or else be complexed by organics (and hence still likely be extracted by AGMP-1). Likewise, one could postulate an oxidation and release of complexed Cr(III) and V(IV), but the oxidized oxyanions should still be extracted by AGMP-1. We are thus left with no satisfying explanation for this decrease in these two elements in the AGMP-1-extractable phase. That this decrease occurred rapidly and in both light and dark bags suggests that removal of either bacteria or particle surfaces by the initial 0.22-μm filtration during collection of the Pearl River water resulted in these changes.

Cobalt and nickel—Co (Fig. 9) and Ni were unique in their behaviors in that neither showed a change in the size fractionation (light and dark bags) during the incubation, yet both showed changes in their chemical fractionation. Co and Ni were both mainly in the dissolved fraction. Each element had significant concentrations in both of the chemical fractions. During the incubation experiment, each was unchanged in dark-bag chemical fractionation. However, in the light bags, both Co and Ni showed significant

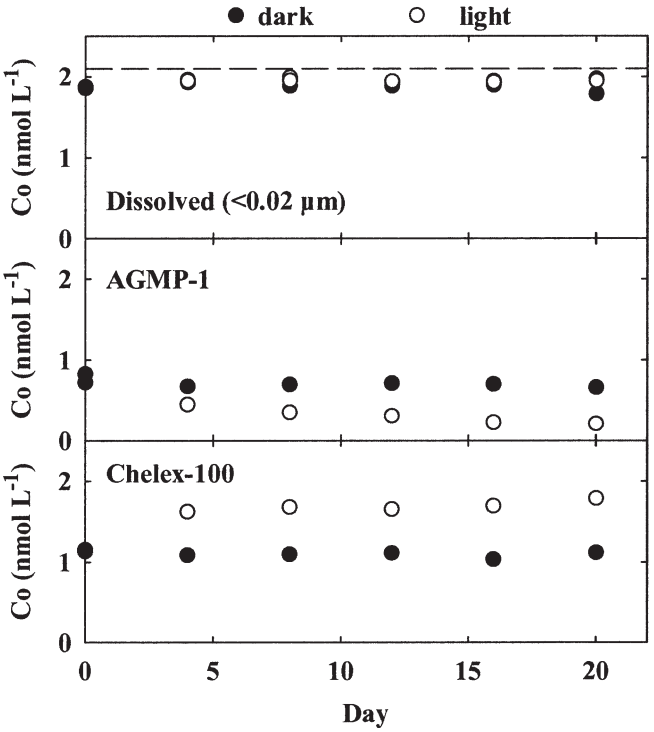

Fig. 9. Cobalt speciation during incubation experiment. The dashed line in the top figure is total concentration (<0.22 μm).

decreases in AGMP-1 fraction with similar increases in the Chelex-100 fraction. For both elements, the 20-d change in concentration in these chemical fractions amounted to about 20% of their total concentrations. This behavior implies that Co and Ni were significantly complexed by LMW organic matter in Pearl River water and that with photodegradation of this DOC, the two elements were released to inorganic or weak organic complexes. Because of the 0.22-μm prefiltration of the Pearl River water prior to the experiment, no particles other than colloids were available in the experiment for surface adsorption. In unfiltered river water, it is possible that some amount of the photoreleased Co and Ni would have been adsorbed by particle surfaces, further changing the physical–chemical speciation of these elements. Additionally, because the AGMP-1 may have retained some amount of inorganic colloidal FeOOH (as discussed previously), it is possible that the photorelease of Co and Ni determined here is a minimum estimate.

Unreactive trace elements—The alkali and alkaline earth metals (Li, Rb, Cs, Sr, and Ba) were all predominantly in the <0.02-μm size fraction; and all predominantly in the Chelex-extractable chemical fraction. Furthermore, none of these elements showed any significant redistribution among size or chemical fractions during the incubation experiment. The physical–chemical fractionation of these elements suggests that they were not complexed by organic matter, and thus their lack of redistribution during the incubation experiment is not surprising.

Tl, Mn, Zn, and Cd were likewise unchanged during the experiments. (The significant AGMP-1 light-bag Mn decrease shown in Table 1 accounts for only a fraction of a percent of total Mn.) For Zn in particular, which is known to be significantly complexed by DOC in some natural waters (e.g., Xue and Sigg 1994) as well as sorbed onto FeOOH (e.g., Dzombak and Morel 1990), the lack of reactivity in our photodegradation experiment is surprising. However, our data indicate that most of the Zn in this Pearl River water is in ionic or weakly complexed forms (Chelex-100; Table 1), in general agreement with the observations of Xue and Sigg (1994). This differs from other cationic metals that did show changes related to photodegradation and that had significant AGMP-1-extractable fractions. Thus, Zn in this river seems to be in a form not conducive to the effects of photodegradation of the DOC (i.e., not in strong organic complexes). Likewise, the other cationic elements dominantly extracted by Chelex-100 were also unreactive in this photodegradation experiment.

The observation of constancy in dissolved Mn during the 3-week incubation is also significant in another context. Shiller and Stephens (2005) found significant microbial removal of dissolved Mn from Pearl River water in less than a day. Thus, the lack of dissolved Mn removal during the 3-week incubation experiment is another indicator of the efficacy of the initial sterile filtration in limiting biological activity.

Mo, Re, and As also showed no significant temporal changes, although in contrast to the alkali and alkaline earth metals, these elements were mainly in the AGMP-1 chemical fraction, most likely reflecting a predominantly anionic inorganic speciation. (Note that Re concentrations were $\sim$2 pmol L^{-1} and Mo concentrations were $\sim$0.3 nmol L^{-1}, both of which are close to the respective detection limits of those two elements; it is thus unlikely we would have been able to observe any changes in the distributions of these elements.)

Implications for fluvial trace element transport—The most basic conclusion of this work is that long-term exposure to sunlight can cause changes in trace element speciation in natural waters. The data indicate a scenario in which photodegradation of LMW DOM releases complexed Fe, which subsequently precipitates as colloidal FeOOH. In this same photodegradation process, other strongly complexed trace elements also appear to be released from organics and then are either adsorbed onto particles and colloids or weakly complexed in solution. Furthermore, because the relative change in dissolved Fe was about twice as large as the relative change in DOC, photodegradation must be affecting both the amount and the molar complexing capacity of the DOM.

This experiment also suggests a difference in what photochemistry does to metal cycling on different timescales. Specifically, on diel timescales, photo-induced changes in metal oxidation state are important, whereas on longer timescales the effect of photodegradation of organic complexers is the important process. This difference in what happens on short and long timescales probably results from two main factors. First, organic compounds are irreversibly altered or destroyed by

photochemical processes. In contrast, metals are reversibly cycled between oxidation states and phases, and are only lost from the system if transferred to a settling particle. Second, because fluvial DOC concentrations are typically an order of magnitude or more greater than the concentrations of Fe and other trace elements, measurable degradation of DOC will proceed more slowly than metal cycling even if the two processes proceed at similar molar rates.

The DOM results indicate that, for this system, it is the LMW organic matter (<1 kDa) that is photodegraded. Furthermore, the breakdown of DCAA to DFAA is evidence for the photodegradation of biologically labile DOC and DON. And the lack of formation of NPAAs despite significant decreases in DOC and increases in DFAA lends confidence to our approach of using sterile filtration to minimize biological activity.

Our results indicate that as DOM becomes more photorefractory with time in a river system (e.g., Molot and Dillon 1997; Kohler et al. 2002), there should be observable changes in metal speciation. Low-order streams with fresh allochthonous DOM inputs and floodplain rivers dominated by photorefractory DOM should have fundamental differences in metal speciation, transport, and bioavailability. Specifically, strong complexation should be a more important factor in rivers and streams with photofresh DOM inputs, whereas adsorption and weak complexation should be more important for streams and rivers with more degraded DOM. This pattern is likely affected by factors such as prolonged photodegradation in oligotrophic lakes and reservoirs, light limitation due to high suspended loads (Miller and Zepp 1979), differences in the inherent complexing ability and reactivity of DOM produced in different environments, as well as the input of photofresh organic matter from downstream wetlands. Furthermore, the divergent DOM degradation results observed by various workers (i.e., preferential loss of low- or high-molecular-weight components) remains an important unanswered problem in fluvial carbon cycling with probable impact on this issue of changing metal speciation in response to photodegradation of organic matter. That Fe(III) can catalyze the photodegradation of organic matter (e.g., Voelker and Sulzberger 1996; Gao and Zepp 1998) additionally emphasizes the feedbacks between metal speciation and DOM photodegradation.

References

Barbeau, K., E. L. Rue, C. G. Trick, K. W. Bruland, and A. Butler. 2003. Photochemical reactivity of siderophores produced by marine heterotrophic bacteria and cyanobacteria based on characteristic Fe(III) binding groups. Limnol. Oceanogr. **43:** 1069–1078.

Bruland, K. W., and M. C. Lohan. 2003. Controls of trace metals in seawater, p. 23–49. *In* H. Elderfield [ed.], Treatise on geochemistry, v. 6: The oceans and marine geochemistry. Elsevier.

Bushaw, K. L., and others. 1996. Photochemical release of biologically available nitrogen from aquatic dissolved organic matter. Nature **381:** 404–407.

Chin, Y.-P., G. Aikin, and E. O'loughlin. 1994. Molecular weight, polydispersity, and spectroscopic properties of aquatic humic substances. Environ. Sci. Technol. **28:** 1853–1858.

Collienne, R. H. 1983. Photoreduction of iron in the epilimnion of acidic lakes. Limnol. Oceanogr. **28:** 83–100.

Cowie, G. L., and J. I. Hedges. 1994. Biochemical indicators of diagenetic alteration in natural organic matter mixtures. Nature **369:** 304–307.

———, J. I. Hedges, and S. E. Calvert. 1992. Sources and relative reactivities of amino acids, neutral sugars, and lignin in an intermittently anoxic marine environment. Geochim. Cosmochim. Acta **56:** 1963–1978.

De Haan, H. 1993. Solar UV-light penetration and photodegradation of humic substances in peaty lake water. Limnol. Oceanogr. **38:** 1072–1076.

Dzombak, D. A., and F. M. M. Morel. 1990. Surface complexation modeling. Wiley.

Emmenegger, L., R. Schönenberger, L. Sigg, and B. Sulzberger. 2001. Light-induced redox cycling of iron in circumneutral lakes. Limnol. Oceanogr. **46:** 49–61.

Gaillardet, J., J. Viers, and B. Dupré. 2003. Trace elements in river waters, p. 225–272. *In* J. I. Drever [ed.], Treatise on geochemistry, v. 5: Surface and ground water, weathering, and soils. Elsevier.

Gao, H., and R. G. Zepp. 1998. Factors influencing photoreactions of dissolved organic matter in a coastal river of the southeastern United States. Environ. Sci. Technol. **32:** 2940–2946.

Jiann, K.-T., and B. J. Presley. 2002. Preservation and determination of trace metal partitioning in river water by a two-column ion exchange method. Anal. Chem. **74:** 4716–4724.

Kieber, R. J., X. Zhou, and K. Mopper. 1990. Formation of carbonyl compounds from UV-induced photodegradation of humic substances in natural waters: Fate of riverine carbon in the sea. Limnol. Oceanogr. **35:** 1503–1515.

Kiel, R. G., E. Tsamakis, J. C. Giddings, and J. I. Hedges. 1998. Biochemical distributions (amino acids, neutral sugars, and lignin phenols) among size classes of modern marine sediments from the Washington coast. Geochim. Cosmochim. Acta **62:** 1347–1364.

King, D. W., H. A. Lounsbury, and F. J. Millero. 1995. Rates and mechanism of Fe(II) oxidation at nanomolar total iron concentrations. Environ. Sci. Technol. **29:** 818–824.

Kirk, J. T. O. 1994. Light and photosynthesis in aquatic ecosystems, 2nd ed. Cambridge Univ. Press.

Kohler, S., I. Buffam, A. Jonsson, and K. Bishop. 2002. Photochemical and microbial processing of stream and soil water dissolved organic matter in a boreal forested catchment in northern Sweden. Aquat. Sci. **64:** 269–281.

Lee, C., and N. O. G. Jørgensen. 1995. Seasonal cycling of putrescine and amino-acids in relation to biological production on a stratified coastal salt pond. Biogeochemistry **2:** 131–157.

Lindim, C., A. M. Mota, and M. L. S. Gonçalves. 2000. Influence of UV-B irradiation in lead speciation from an estuarine sample. Water Res. **34:** 3325–3334.

Liu, X. W., and F. J. Millero. 1999. The solubility of iron hydroxide in sodium chloride solutions. Geochim. Cosmochim. Acta **63:** 3487–3497.

Lyven, B., M. Hassellov, D. R. Turner, C. Haraldsson, and K. Andersson. 2003. Competition between iron- and carbon-based colloidal carriers for trace metals in a freshwater assessed using flow field-flow fractionation coupled to ICPMS. Geochim. Cosmochim. Acta **67:** 3791–3802.

Martell, A. E., and R. M. Smith. 1995. Critical stability constants. National Institute of Standards and Technology Standard Reference Database 46, Version 2.0., NIST: Gaithersburg, MD.

Miles, C. J., and P. L. Brezonik. 1981. Oxygen consumption in humic-colored waters by a photochemical ferrous-ferric catalytic cycle. Environ. Sci. Tech. **15:** 1089–1095.

Miller, G. C., and R. G. Zepp. 1979. Effects of suspended sediments on photolysis rates of dissolved pollutants. Water Res. **13:** 543–549.

Miller, W. L., and R. G. Zepp. 1995. Photochemical production of dissolved inorganic carbon from terrestrial organic matter: Significance to the oceanic organic carbon cycle. Geophys. Res. Lett. **22:** 417–420.

Millero, F. J., and S. Sotolongo. 1989. The oxidation of Fe(II) with H_2O_2 in seawater. Geochim. Cosmochim. Acta **53:** 1867–1873.

———, S. Sotolongo, and M. Izaguirre. 1987. The kinetics of oxidation of Fe(II) in seawater. Geochim. Cosmochim. Acta **51:** 793–801.

Moffett, J. W., and R. G. Zika. 1988. Measurement of copper(I) in surface waters of the subtropical Atlantic and Gulf of Mexico. Geochim. Cosmochim. Acta **52:** 1849–1857.

Molot, L. A., and P. J. Dillon. 1997. Photolytic regulation of dissolved organic carbon in northern lakes. Global Biogeochem. Cycles **11:** 357–365.

Moran, M. A., and R. G. Zepp. 1997. Role of photoreactions in formation of biologically labile compounds from dissolved organic matter. Limnol. Oceanogr. **42:** 1307–1316.

Morris, D. P., and B. R. Hargreaves. 1997. The role of photochemical degradation of dissolved organic carbon in regulating the UV transparency of three lakes on the Pocono Plateau. Limnol. Oceanogr. **42:** 239–249.

Orem, W. H., P. G. Hatcher, E. C. Spiker, N. M. Szeverenyi, and G. E. Maciel. 1986. Dissolved organic matter in anoxic pore waters from Mangrove Lake, Bermuda. Geochim. Cosmochim. Acta **50:** 609–618.

Osburn, C. L., D. P. Morris, K. A. Thorn, and R. E. Moeller. 2001. Chemical and optical changes in freshwater dissolved organic matter exposed to solar radiation. Biogeochem. **54:** 251–278.

Patel-Sorrentino, N., S. Mounier, Y. Lucas, and J. Y. Benaim. 2004. Effects of UV-visible irradiation on natural organic matter from the Amazon basin. Sci. Total Environ. **321:** 231–239.

Pokrovsky, O. S., and J. Schott. 2002. Iron colloids/organic matter associated transport of major and trace elements in small boreal rivers and their estuaries (NW Russia). Chem. Geol. **190:** 141–179.

Powell, R. T., and A. Wilson-Finelli. 2003. Photochemical degradation of organic iron complexing ligands in seawater. Aquat. Sci. **65:** 367–374.

Reuter, J. H., and E. M. Perdue. 1977. Importance of heavy metal-organic solute interactions in natural waters. Geochim. Cosmochim. Acta **41:** 325–334.

Rush, J. D., and B. H. J. Bielski. 1985. Pulse radiolytic studies of the reactions of HO_2/O_2^- with Fe(II)/Fe(III) ions. The reactivity of HO_2/O_2^- with ferric ions and its implication on the occurrence of the Haber-Weiss reaction. J. Phys. Chem. **89:** 5062–5066.

Sander, S., J. P. Kim, B. Anderson, and K. A. Hunter. 2005. Effect of UVB irradiation on Cu^{2+}-binding organic ligands and Cu^{2+} speciation in alpine lake waters of New Zealand. Environ. Chem. **2:** 56–62.

Shiller, A. M. 2003. Syringe filtration methods for examining dissolved and colloidal trace element distributions in remote field locations. Environ. Sci. Technol. **37:** 3953–3957.

———, and T. H. Stephens. 2005. Microbial manganese oxidation in the lower Mississippi River: Methods and evidence. Geomicrobiol. J. **22:** 117–125.

Tarr, M. A., W. Wang, T. S. Bianchi, and E. Engelhaupt. 2001. Mechanisms of ammonia and amino acid photoproduction from aquatic humic and colloidal matter. Water Res. **35:** 3688–3696.

Theis, T. L., and P. C. Singer. 1974. Complexation of iron(II) by organic matter and its effect on iron(II) oxygenation. Environ. Sci. Technol. **8:** 569–573.

Tranvik, L., and S. Bertilsson. 2001. Contrasting effects of solar UV radiation on dissolved organic sources for bacterial growth. Ecol. Lett. **4:** 458–463.

Twardowski, M. S., and P. L. Donaghay. 2002. Photobleaching of aquatic dissolved materials: Absorption removal, spectral alteration, and their interrelationship. J. Geophys. Res. Oceans **107** (C8). [doi: 10.1029/1999JCOO281]

Voelker, B., F. M. M. Morel, and B. Sulzberger. 1997. Iron redox cycling in surface waters: Effects of humic substances and light. Environ. Sci. Technol. **31:** 1004–1011.

Voelker, B. M., and B. Sulzberger. 1996. Effects of fulvic acid on Fe(II) oxidation by hydrogen peroxide. Environ. Sci. Technol. **30:** 1106–1114.

Waite, T. D., and F. M. M. Morel. 1984. Photoreductive dissolution of colloidal iron oxides in natural waters. Environ. Sci. Technol. **18:** 860–868.

Weishaar, J. L., G. R. Aiken, B. A. Bergamaschi, M. S. Fram, R. Fujii, and K. Mopper. 2003. Evaluation of specific ultraviolet absorbance as an indicator of the chemical composition and reactivity of dissolved organic carbon. Environ. Sci. Technol. **37:** 4702–4708.

Wetzel, R. G., P. G. Hatcher, and T. S. Bianchi. 1995. Natural photolysis by ultraviolet irradiance of recalcitrant organic matter to simple substrates for rapid bacterial metabolism. Limnol. Oceanogr. **40:** 1369–1380.

Xie, H., O. C. Zafiriou, W.-J. Cai, R. G. Zepp, and Y. Wang. 2004. Photooxidation and its effects on the carbonyl content of dissolved organic matter in two coastal rivers in the southeastern United States. Environ. Sci. Technol. **38:** 4113–4119.

Xue, H. B., and L. Sigg. 1994. Zinc speciation in lake waters and its determination by ligand-exchange with EDTA and differential-pulse anodic-stripping voltammetry. Analyt. Chim. Acta **284:** 505–515.

Yuan, J. 2000. The distribution of hydrogen peroxide in seawater of the central Atlantic Ocean and in river waters of southern Mississippi and Louisiana. Ph.D. dissertation, Univ. of Southern Mississippi.

Received: 11 August 2005
Accepted: 6 February 2006
Amended: 13 March 2006